World Conference on Timber Engineering Oslo 2023

ESTIMATION OF MOISTURE DISTRIBUTION IN SAWN TIMBER USING COMPUTED TOMOGRAPHY

Boris Poupet[1], José Couceiro[1], Sara Florisson[2], Lars Hansson[3], Dick Sandberg[1]

ABSTRACT: Most of the physical, mechanical, and esthetic properties of wood products are affected by the drying of sawn timber. A better understanding of moisture transport in wood during kiln drying is necessary to obtain better quality products, shorter drying schedules, lower energy consumption, and a more sustainable process. Four-dimensional X-ray computed tomography (4DCT) (three-dimensional in space and one in time) with image processing techniques can be used to study the moisture content (MC) of sawn timber during kiln drying. The development of the technique is however made difficult by computational complexity and a lack of accurate experimental validation. In this study, a method relying on 4DCT has been developed using state-of-the-art image processing techniques. The method was validated by a regression analysis of the predicted MC against gravimetric measurements for different timber cross sections and different initial MC distributions on a significantly smaller scale than has previously been investigated. It is concluded that the MC can be estimated with an average uncertainty of ±4.8 percentage points on a 10 mm scale. Sawmills could ultimately benefit from a better understanding of wood-water interactions and dry sawn timber more efficiently.

KEYWORDS: four-dimensional, drying, moisture content, elastic-image registration, Norway spruce

1 INTRODUCTION

Wood is a hygroscopic material that attracts and holds water through adsorption from the surrounding environment, but wood-water interactions are still not fully understood [1], Swedish sawmills thus use software based on numerical models dating back to the mid-eighties to determine drying schedules for timber [2]. It has been empirically shown that shorter schedules are possible, reducing energy consumption and time.

X-ray computed tomography is being used in Swedish sawmills to study logs and timber in a non-destructive manner. The investigation of the internal structure of wood by means of tomography started in the mid-eighties with a medical CT scanner with first studies focused on determining the moisture content (MC) through image processing [3]. Since then, several methods have been developed to study the MC distribution with increasing complexity: unidimensional along radial lines [4], two-dimensional by manually deforming tomograms [5] digital image correlation [6], and two-dimensional in time with image registration [7].

However, almost four decades after the first investigations to determine the MC from tomograms, no attempts have been made to expand the idea to four dimensions, i.e., processing volumetric tomographic data repetitively acquired during a certain period. Such a method would be useful to investigate e.g., moisture transport along the fibres, and moisture-induced deformations in the sawn timber. Two-dimensional methods were previously usually validated against a gravimetric reference by averaging the MC determined through CT (predicted MC) of the entire cross-section [8], although this did not allow to assess the reliability of the method on a small scale.

This study contributes to the development of an image processing method to efficiently compute the MC distribution from 4DCT data. The method is validated to quantify its accuracy and precision against a gravimetric reference on a centimetre scale.

2 MATERIALS AND METHODS

2.1 Specimen preparation

Two undried centre-yield planks of Norway spruce (*Picea abies*) were collected in a local sawmill in northern Sweden. One plank, labelled S40, had a green cross-

[1] Division of Wood Science and Engineering, Department of Engineering Sciences and Mathematics, Luleå University of Technology, Sweden, boris.poupet@ltu.se
[2] Department of Materials Science and Engineering, Division of Applied Mechanics, Uppsala University, Sweden, sara.florisson@angstrom.uu.se
[3] Department of Ocean Operations and Civil Engineering, Faculty of Engineering, Norwegian University of Science and Technology, 6025 Ålesund, Norway, laha@ntnu.no

https://doi.org/10.52202/069179-0104

sectional area of 40×160 mm², and the other, labelled S70, 70×160 mm²; both with a length of approx. 5 m. From each plank, three specimens with a length of 200 mm containing only clear wood were cut, sealed on their exposed cross-sections with a layer of silicone Casco SuperFix+ [Sika, Baar, Switzerland], wrapped in plastic film and stored in a frozen condition to limit uncontrolled drying before the start of the experiments.

2.2 Validation

The MC computation from CT data was studied with different MC distributions achieved in three different ways: (1) with no drying (i.e., in the green condition), (2) by drying at 70°C for 1 h, and (3) by drying at 70°C for 3 h. The silicone on the end grain impeded longitudinal moisture transport to obtain MC distributions like those obtained with industrial kilns. After the treatment, two adjacent clear wood samples with a thickness of 20 mm were cut from each specimen, one labelled "CT" and the other "reference". On the exposed cross section of the reference samples, horizontal and vertical lines were drawn at centimetre intervals to form a regular grid (Figure 1).

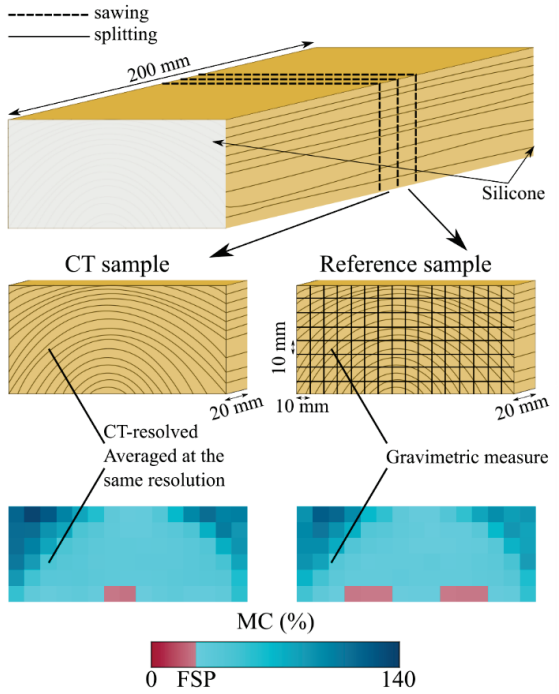

Figure 1: *CT and reference samples prepared after the specimen treatment. The MC distribution of the reference sample was determined gravimetrically by splitting it into test volumes 10 mm×10 mm×20 mm in size. The MC distribution in the CT sample was predicted with the CT method and averaged at the same spatial resolution.*

The CT sample was used to obtain the 2D density distribution ρ_{CT} after drying using a Siemens Somatom Emotion Duo [Siemens, Munich, Germany] CT-scanner at a spatial resolution of 0.98 mm×0.98 mm in the cross-sectional plane and 10 mm lengthwise. The masses after treatment of both CT and reference samples were acquired with a precision balance Ohaus AX523 [Ohaus, Parsippany, USA]. The reference samples were split with a knife along the grid lines into test volumes 10 mm×10 mm×20 mm in size and their initial masses were determined with the precision balance. The samples were oven-dried at 103±2°C (CEN 2002) and reweighed. The CT sample was rescanned with the same settings to evaluate its oven-dry density distribution $\rho_{0,CT}$.

In the reference samples, the gravimetric MC of the jth test volume (w_g^j) was computed using Equation (1):

$$w_g^j = \frac{m_i^j - m_0^j}{m_0^j} \quad (1)$$

where m_i^j is the initial mass of the jth test volume and m_0^j its oven-dry mass. Together, the measures w_g^j form the MC distribution w_g of the reference sample. The MC of the CT sample w_{CT} was predicted on the voxel scale using the method described in 1.3. For comparison with the reference MC distribution, the predicted MC was averaged in test volumes of 10 mm×10 mm×10 mm as w_{CT}^j.

Although these experiments use the 4DCT method to provide the first validation of the method, it was performed in 2D to simplify the process. It was observed in preliminary tests that the cross-sectional directions of the wood are the most troublesome to register. The gravimetric method to which the predicted MC is validated is very time-consuming, it would not be practical to repeatedly implement it for many CT/reference sample pairs contained in the same specimen.

2.3 Image processing

The image processing method was intended for use with 4DCT data, but it is applicable in fewer dimensions. Regardless of the dimensions, data reconstructed by the CT scanner are stacked as a density field in NRRD format. Processing this density data for MC computation involves three steps: image registration, density correction, and MC calculation.

2.3.1 Image registration

To compute the change in MC during drying, the density fields $\rho(\mathbf{X},t)$ at different times (t) must be compared to the oven-dry density field $\rho_0(\mathbf{x})$, where $\mathbf{X} = (X,Y,Z)$ are the material coordinates and $\mathbf{x} = (x,y,z)$ are the spatial coordinates as shown in Figure 2. This operation is made difficult by the anisotropic deformations that sawn timber undergoes while drying, which introduce misalignments between the tomograms. To solve this problem, state-of-the-art elastic image registration based on B-splines was used [9]. This technique computes a coordinate transformation from the material to the spatial coordinates $\mathbf{x} = \mathbf{T}(\mathbf{X},t)$ so that the registered densities $\rho(\mathbf{x},t)$ are spatially aligned with $\rho_0(\mathbf{x})$, as illustrated in Figure 2. The registration is performed in the image-analysis software *3Dslicer* using the *Sequence Registration* module

specially dedicated to 4D registration based on the *Elastix* toolbox [9]. With the different input data tested, the algorithm always converged to a solution as long as the deformations were continuous, i.e., provided that no cracks or material losses occurred.

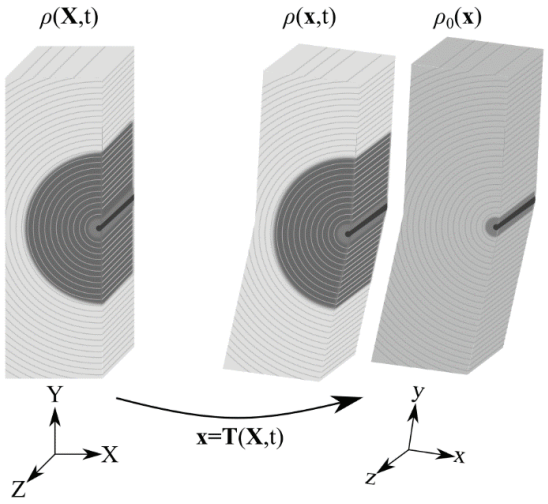

Figure 2: *Lagrangian description of the displacement experienced by a wood volume from an undeformed configuration* $\boldsymbol{\rho(X,t)}$ *to a deformed configuration (oven-dry)* $\boldsymbol{\rho_0(x)}$*. By applying the transformation* $\mathbf{T}(\mathbf{X},t)$*, the volumes become spatially aligned (shifted in the illustration by a rigid-body displacement for visualisation purposes).*

2.3.2 Density correction

The registered densities $\rho(\mathbf{x},t)$ must be interpolated and recalculated. The transformation performed by the image registration allocates the registered densities to non-voxel positions, and interpolation is necessary to assign a single density value to each voxel position. Since the image registration deforms the wood volume, the densities must be recalculated to compensate for the local volumetric strains defined by Equation (2).

$$\varepsilon_V(\mathbf{x},t) = \frac{V_0(\mathbf{x}) - V(\mathbf{X},t)}{V_0(\mathbf{x})} \tag{2}$$

Where $V(\mathbf{X},t)$ is the voxel volume in the undeformed configuration and $V_0(\mathbf{x})$ is its equivalent in the deformed configuration.

Density interpolation and rescaling were performed simultaneously with an algorithm developed by Hansson and Fjellner [10] and based on polygon clipping. The volumetric strain was decomposed as the sum of the elementary strains $\varepsilon_V = \Sigma\varepsilon_j$ computed in the regions enclosed by the undeformed grid. The rescaled densities $\rho'(\mathbf{x},t)$ were computed as shown in Figure 3 using Matlab® [MathWorks, Natick, USA].

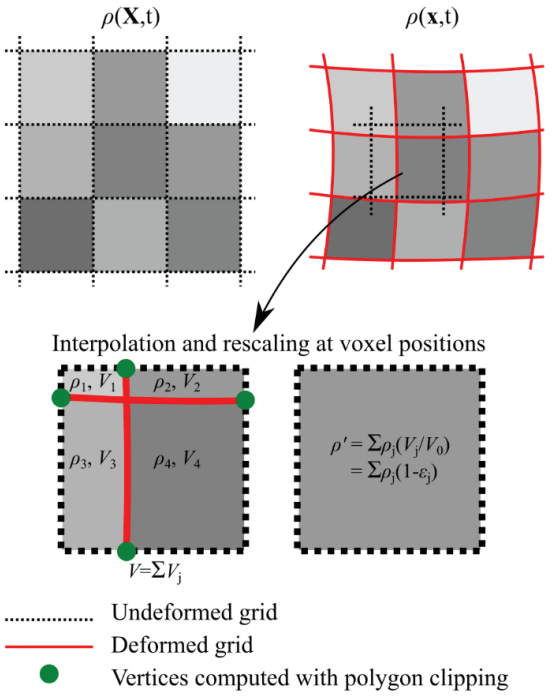

Figure 3: *Density correction. The volumes* V_j *are computed by obtaining the vertex coordinates via polygon clipping. The rescaled density is the sum of the densities weighted by their respective volumetric changes. The illustration is limited to 2D for visualization purposes.*

2.3.3 Moisture content calculation

The MC was computed using Matlab® at the voxel level from the spatial coordinates in Equation (3):

$$w(\mathbf{x},t) = \frac{\rho'(\mathbf{x},t) - \rho_0(\mathbf{x})}{\rho_0(\mathbf{x})} \tag{3}$$

2.4 Uncertainties of measurement and errors

Differences between the gravimetric (w_g) and predicted (w_{CT}) MC distributions were studied with respect to measurement limitations and errors to estimate the uncertainty of the method.

The uncertainty of the gravimetric method u_g^j was estimated in Equation (4) for each test volume as the combined uncertainty of measurement due to the scale precision u_s^j and uncertainty due to the ongoing drying of the reference samples while being splitted (u_d).

$$u_g^j = \sqrt{\left(u_s^j\right)^2 + {u_d}^2} \tag{4}$$

The precision of the balance is given by the manufacturer as $\Delta m = \pm 10^{-6}$ kg. The uncertainty u_s^j is computed in Equation (5) as the total differential of w_g^j defined in Equation (1).

https://doi.org/10.52202/069179-0104

$$u_{\mathrm{s}}^{\mathrm{j}} = \frac{\Delta m}{m_0^{\mathrm{j}}}\left(2 + w_{\mathrm{g}}^{\mathrm{j}}\right) \tag{5}$$

The uncertainty u_{d} is estimated for each reference sample in Equation (6):

$$u_{\mathrm{d}} = w_{\mu}\left(m_{\mathrm{i}}, \Sigma m_0^{\mathrm{j}}\right) - w_{\mu}\left(\Sigma m_{\mathrm{i}}^{\mathrm{j}}, \Sigma m_0^{\mathrm{j}}\right) \tag{6}$$

where $w_{\mu}\left(m_{\mathrm{i}}, \Sigma m_0^{\mathrm{j}}\right)$ is the average MC of the reference sample with initial mass m_{i}, and $w_{\mu}\left(\Sigma m_{\mathrm{i}}^{\mathrm{j}}, \Sigma m_0^{\mathrm{j}}\right)$ its average MC based on the initial mass $\Sigma m_{\mathrm{i}}^{\mathrm{j}}$, i.e., the sum of the initial masses of the test volumes. In both situations, the oven-dry mass was assumed to be Σm_0^{j}, i.e., the sum of the oven-dry masses of each test volume, as the oven-dry masses of the reference samples could not be measured before the splitting.

The uncertainty of the predicted MC ($u_{\mathrm{CT}}^{\mathrm{j}}$) is estimated for each test volume from Equation (7) as the combined uncertainty due to the density measurement of the CT-scanner u_{ρ}^{j} and the errors associated with the image processing steps $u_{\mathrm{im}}^{\mathrm{j}}$:

$$u_{\mathrm{CT}}^{\mathrm{j}} = \sqrt{\left(u_{\rho}^{\mathrm{j}}\right)^2 + \left(u_{\mathrm{im}}^{\mathrm{j}}\right)^2} \tag{7}$$

The precision of density measurement by the CT scanner was taken to be $\Delta\rho_{\mathrm{CT}} = \pm 4$ kg/m³. This value corresponds to the scatter of the density distribution measured for a 1 cm³ volume of a water phantom at thermal equilibrium with a 95% confidence interval.

This uncertainty was propagated by computing the total differential of w_{CT} and estimated for each voxel in Equation (8):

$$u_{\rho} = \frac{\Delta\rho_{\mathrm{CT}}}{\rho_{0,\mathrm{CT}}}\left(2 + w_{\mathrm{CT}}\right) \tag{8}$$

This uncertainty was sufficiently uniform in the capillary and bound water dominated regions to justify averaging the values according to Equation (9):

$$u_{\rho}^{\mathrm{j}} = \begin{cases} u_{\rho,\mathrm{c}}\,, w_{\mathrm{CT}}^{\mathrm{j}} > 0.6 \\ u_{\rho,\mathrm{b}}\,, w_{\mathrm{CT}}^{\mathrm{j}} \leq 0.6 \end{cases} \tag{9}$$

where $u_{\rho,\mathrm{c}}$ and $u_{\rho,\mathrm{b}}$ are the average uncertainties of the capillary and bound water dominated regions respectively.

The uncertainty $\Delta_{\mathrm{z}} w$ accounts for the differences in MC between the CT and reference samples, i.e., the lengthwise gradients of MC, as:

$$\Delta_{\mathrm{z}} w = w_{\mu,\mathrm{CT}} - w_{\mu,\mathrm{r}} \tag{10}$$

where $w_{\mu,\mathrm{CT}}$ and $w_{\mu,\mathrm{r}}$ are the average gravimetric MCs of the CT and reference samples respectively.

The absolute difference between the predicted MC and the gravimetric MC is interpreted as being the combined uncertainty due to the gravimetric method, the CT method, and experimental limitations:

$$\left|w_{\mathrm{g}} - w_{\mathrm{CT}}\right| = \sqrt{{u_{\mathrm{g}}}^2 + {u_{\mathrm{CT}}}^2 + \left(\Delta_{\mathrm{z}}^{\mathrm{j}} w\right)^2} \tag{11}$$

The uncertainty $u_{\mathrm{im}}^{\mathrm{j}}$ corresponding to the errors due to the image processing was not directly estimated in this study but was instead indirectly evaluated in Equation (12) by comparing the observed difference between the CT and reference MC distributions and the previously evaluated uncertainties.

$$u_{\mathrm{im}}^{\mathrm{j}} = \sqrt{\left(w_{\mathrm{g}}^{\mathrm{j}} - w_{\mathrm{CT}}^{\mathrm{j}}\right)^2 - \left(u_{\rho}^{\mathrm{j}}\right)^2 - \left(u_{\mathrm{g}}^{\mathrm{j}}\right)^2 - \left(\Delta_{\mathrm{z}} w\right)^2} \tag{12}$$

Lindgren et al. [3] determined experimentally a maximal deviation of 2 pixels when performing a non-linear transformation for a wood sample between an equilibrium MC state and a state after soaking the sample in water. These authors related this spatial mismatch to an additional density uncertainty $\Delta\rho_{\mathrm{im}} = \pm 6$ kg/m³, which is higher by a factor of 1.5 than the uncertainty due to the CT-scanner. Under this assumption, a threshold was set to evaluate whether the image registration introduced a spatial mismatch (s^{j}) greater or less than 2 pixels:

$$s^{\mathrm{j}} = \begin{cases} \leq 2 \text{ pixels} & \text{if } u_{\mathrm{im}}^{\mathrm{j}} \leq 1.5 u_{\rho}^{\mathrm{j}} \\ > 2 \text{ pixels} & \text{else} \end{cases} \tag{13}$$

3 Results

Linear regressions between the predicted and gravimetric MCs were calculated and the results are shown in Figure 4. The predicted MC tends to be overestimated, since the regression lines are located above the line of equality $w_{\mathrm{CT}} = w_{\mathrm{g}}$.

The cross-sectional area and the MC distribution of the samples were identified as the parameters which had the greatest impact on the reliability of the image processing method. An increase in the cross-sectional area was indeed expected to increase the computation complexity as more voxels must be processed. The MC distribution was expected to influence the performance of the method, since it is correlated to the degree of deformation of the wood. The MC computation should be more complex in an undeformed configuration (green sawn timber) than in an intermediately deformed configuration (between a green and an oven-dry state).

https://doi.org/10.52202/069179-0104

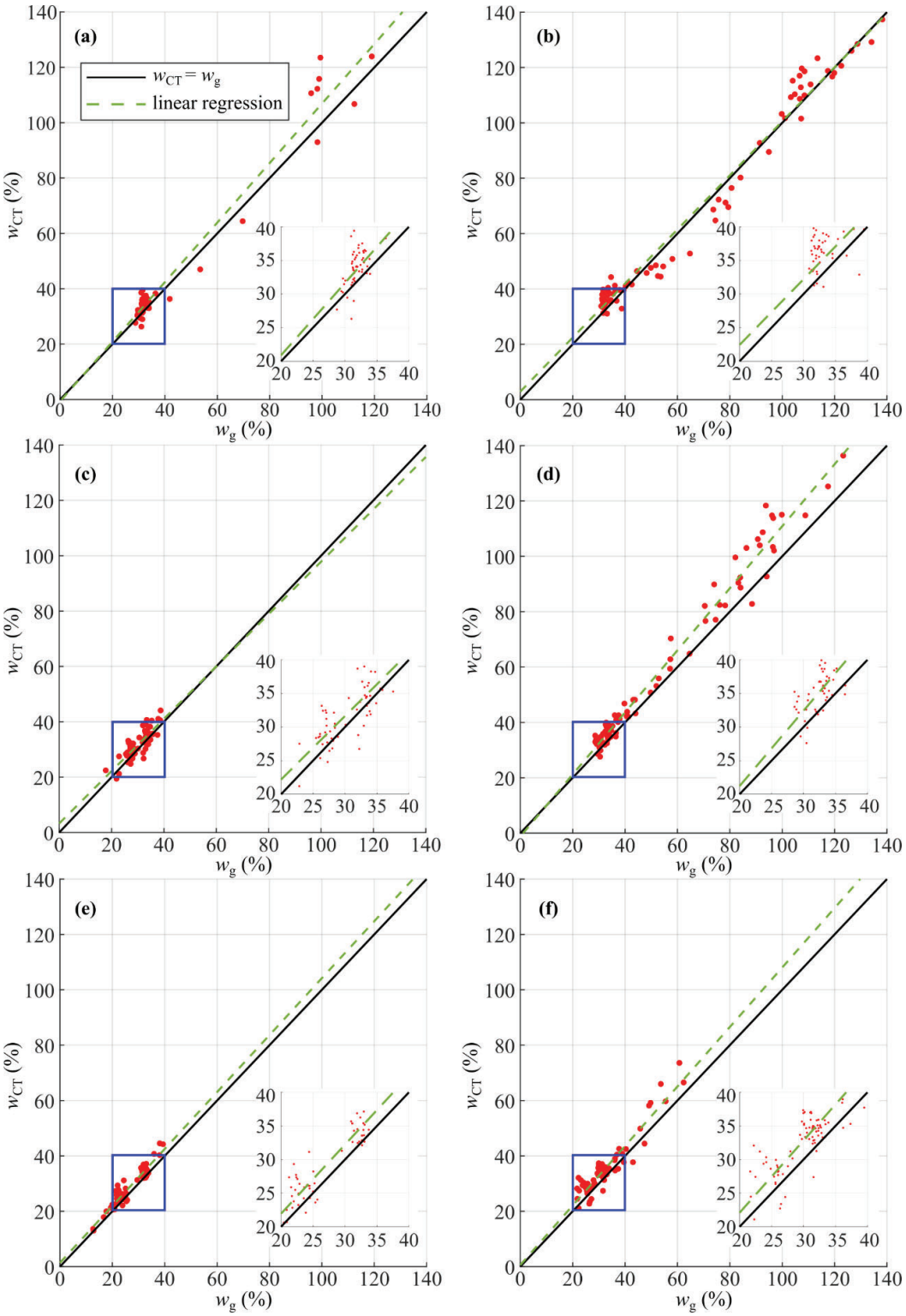

Figure 4: *The predicted MC (w_{CT}) plotted against the gravimetric MC (w_g). (a), (c), and (e) represent the S40 samples with cross-sectional area of 40×160 mm², and (b), (d), and (f) represent the S70 samples with a cross-sectional area of 70×160 mm². (a) and (b) specimens that underwent no drying; (c) and (d) specimens that underwent drying for 1h at 70°C; (e) and (f) specimens that underwent drying for 3h at 70°C. The diagonal plain line represents a perfect match between the two datasets ($w_{CT=}w_g$). The dashed line corresponds to a linear regression. The smaller graph with values from 20 % to 40 % is a region around FSP for better visualization.*

https://doi.org/10.52202/069179-0104

The validation was assessed by the root-mean square error (RMSE) which indicates the precision of the method and the coefficient of determination of the linear regression (R^2) which indicates its accuracy. The results are presented in Figure 5.

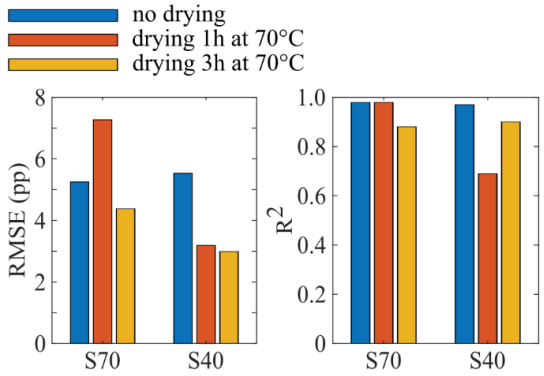

Figure 5: *Precision and accuracy of the CT-method. Root-mean-square-error (left) and R^2 (right) of the linear regressions. "pp" stands for percentage points.*

The average RMSE was higher for the larger S70 specimens than for the smaller S40 specimens, which suggests that a larger cross-sectional area is more complex to process for both image registration and density correction algorithms. The RMSE of the S40 specimens decreased from 5.5 to 3 percentage points (pp) when the drying was extended from 0 h to 3 h. The RMSE of the S70 specimens was 5.25, 7.28, and 4.38 pp for 0 h, 1 h, and 3 h drying respectively. Except for the RMSE peak at 1 h drying for the S70 specimen, these observations suggest that the image processing performs better when the sawn timber is dried, as it is easier to compute smaller deformations. A decrease in the R^2 coefficient was observed for both specimen groups with increasing drying time.

The performance of the image processing method was assessed by quantifying its uncertainty and spatially mapping it within the cross section. The uncertainty was estimated with Equations (12-13) and the results are shown in Figure 6. High uncertainties (>10 pp) considered as outliers were always found for test volumes located at the sample edge, mostly in the sapwood region. Uncertainties corresponding to spatial mismatches greater than 2 pixels (>*) were relatively more frequently found in the S70 than in the S40 samples. Drying lowered the average uncertainty value for both sample sizes.

The occurrence of test volumes with spatial mismatches greater than 2 pixels in CT samples could be related to their respective strain distributions. It was inferred that the image registration was worse for regions experiencing a high strain and shear.

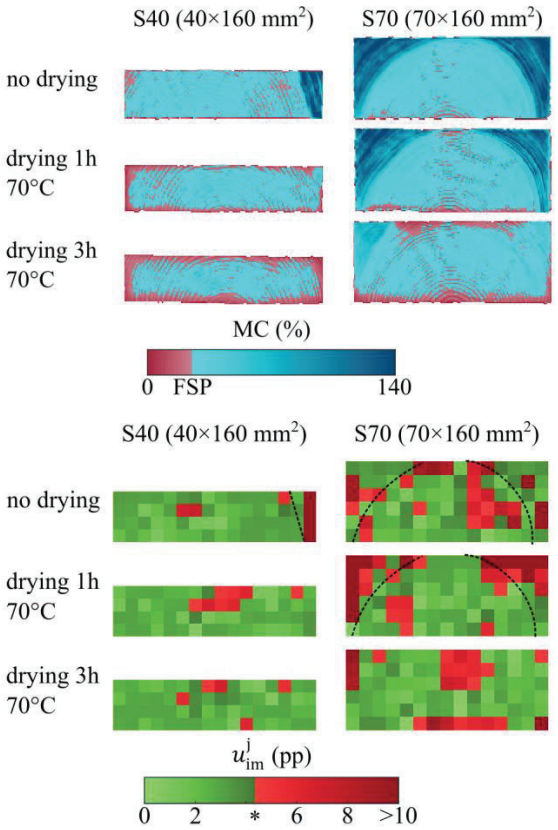

Figure 6: *Predicted MC (top) and uncertainty of the image processing method (below). The threshold marked * is set as described in Equation (13): values below or above it corresponds to spatial mismatches greater or less than 2 pixels. The value of the threshold is slightly different for each situation and ranges from 3.8 to 4.5 pp. The dashed curves indicate the sapwood/heartwood borders when they were visible in the CT data. "pp" stands for percentage points.*

4 CONCLUSIONS

It has been shown that the image processing is a suitable method for the calculation of MC with an average uncertainty ranging from 2.8 to 4.9 pp estimated on a 10 mm scale. A fine adjustment of the image processing parameters might reduce this error. Measurement limitations of the CT scanner increase this range to ±[4.4-7.8] pp, which may be improved by using another image reconstruction algorithm.

The method performed better when the cross section of the specimen was smaller, as the complexity of the image registration decreases with a decreasing amount of data to process. The method was also more precise when the transformation was computed from an intermediate deformed configuration than from an undeformed configuration (green condition). Consequently, the reliability increased with a lower MC, dry enough to initiate the deformation. The cross-sectional area of the specimen was identified as having a greater effect than the MC distribution on the precision of the method.

https://doi.org/10.52202/069179-0104

Extending this method to compute the MC in 4D can be better than existing methods for investigating wood-water relations during the drying of sawn timber, and for other processes such as wood modification or mechanical testing. The method will be expanded to characterize moisture-induced strain fields based on the displacement data obtained by image registration.

ACKNOWLEDGEMENT

The authors acknowledge the considerable support of the CT WOOD research program at Luleå University of Technology in Skellefteå for the development of X-ray computed tomography applications for use in the forest products industry.

REFERENCES

[1] E. E. Thybring, M. Fredriksson, S. L. Zelinka, S. V. Glass. Water in Wood: A Review of Current Understanding and Knowledge Gaps. *Forests,* 13(12):2051, 2022

[2] J. Salin. Simulation models; from a scientific challenge to a kiln operator tool. In *6 th International IUFRO Wood Drying Conference*, pages 25-28, 1999.

[3] O. Lindgren, S. Grundberg, J. R. Davis. Applying digital image processing on CAT-scan images of wood for non-destructive moisture content measurements. Paper VI in *O. Lindgren, 1992. Medical CT-Scanners for Non-Destructive Wood Density and Moisture Content Measurements. Doctoral thesis. Luleå University of Technology, Division of Wood Technology, Skeria 3, SE-931 87 Skellefteå, Sweden. Thesis No. 1992:111D. ISSN 0348-8373,* 1992.

[4] J. R. H. Fromm, I. Sautter, D. Matthies, J. Kremer, P. Schumacher, C. Ganter. Xylem Water Content and Wood Density in Spruce and Oak Trees Detected by High-Resolution Computed Tomography. *Plant Physiology*, 127(2): 416-425, 2001.

[5] C. Lazarescu, K. Watanabe, S. Avramidis. Density and moisture profile evolution during timber drying by CT scanning measurements. *Drying technology,* 28(4): 460-467, 2010.

[6] K. Watanabe, C. Lazarescu, S. Shida, and S. Avramidis. A Novel Method of Measuring Moisture Content Distribution in Timber During Drying Using CT Scanning and Image Processing Techniques. *Drying Technology,* 30(3): 256-262, 2012.

[7] L. Hansson, E. Cherepanova. Determination of wood moisture properties using a CT-scanner in a controlled low-temperature environment. *Wood Material Science and Engineering,* 7(2): 87-92, 2012.

[8] J. Couceiro, D. Elustondo. Implementation of computer aided tool for non-destructive X-ray measurement of moisture content distribution in wood. *Pro Ligno,* 11(4): 330-336, 2015.

[9] S. Klein, M. Staring, K. Murphy, M. A. Viergever, J. Pluim. Elastix: A Toolbox for Intensity-Based Medical Image Registration. *IEEE Transactions on Medical Imaging,* 29(1): 196-205, 2010.

[10] L. Hansson, B-A. Fjellner. Wood shrinkage coefficient and dry weight moisture content estimation from CT-images. *Pro Ligno,* 9(4): 557-561, 2013.

https://doi.org/10.52202/069179-0104